Soft Matter

PAPER

View Article Online
View Journal | View Issue

Cite this: *Soft Matter*, 2015, 11, 6780

Reactive modeling of the initial stages of alkoxysilane polycondensation: effects of precursor molecule structure and solution composition†

Joshua D. Deetz* and Roland Faller

Received 22nd April 2015,
Accepted 20th July 2015

DOI: 10.1039/c5sm00964b

www.rsc.org/softmatter

Reactive molecular dynamics simulations were performed to study the polycondensation of alkoxysilane in solution with alcohol and water. The dynamic formation of siloxane clusters and rings was observed with simulation time. Two mechanisms for the growth of siloxanes were observed: monomer addition and cluster–cluster aggregation. The impacts of the alkoxysilane monomer chemical structure and solution composition on the rates of hydrolysis and condensation were explored. The polycondensation of different precursor alkoxysilane monomers (tetramethoxysilane, trimethoxysilane, methyltrimethoxysilane, or tetraethoxysilane) was modeled. The steric bulk of chemical groups attached to the monomer, such as silyl or alkoxy groups, were found to impact reaction rates. The influence of solution composition was investigated by simulating multiple systems with different concentrations of tetramethoxysilane, methanol, and water. Reactive molecular dynamics is used for the first time to study the polycondensation of alkoxysilanes, creating opportunities for future theoretical studies of the sol–gel process.

I. Introduction

Sol–gel processes[1] are widely used to generate metal-oxide solid materials through the three-dimensional polymerization of monomer molecules. Silicon-based precursor molecules, such as alkoxysilanes, can form silica materials with a variety of applications, such as aerogels,[2–5] bio-active,[6] low dielectric constant[7] materials, and coupling agents between ceramics and polymers.[8] The diverse range of materials that can be formed results from the precursor molecule's ability to hydrolyze, generating silanol chemical groups in the presence of water which subsequently condense to form siloxane linkages.[9] The hydrolysis and condensation reactions are illustrated in Scheme 1.

The chemical structure of alkoxysilanes has been shown to dictate the kinetics of their hydrolysis and condensation,[10–17] manifesting through the steric accessibility[16,17] and polarity[13] of the reacting Si–O bonds. The size of the alkoxide ligands[11,15,17] is one structural property of alkoxysilane precursor monomers that influences their gelation chemistry. Most commonly these groups are methoxy- or ethoxysilanes,[1] although monomers with larger ligands, such as propoxy-,[18] and butoxysilanes[15,19] have also been studied. Increasing the alkoxysilane ligand size leads to longer gelation times[15] and slower kinetics,[11,13,17] suggesting steric hindrance to reactions.

Trialkoxysilanes are available with silyl headgroups[11,17,20] that have diverse chemistries, such as alkyl,[17] mercaptoalkyl,[21] and aminoalkyl[20] headgroups. The headgroup has a strong influence on the reactivity of the monomer,[10,13,16] and the solubility[17] in organic solvent and water, which subsequently dictates the chemical structure of the forming products. Loy *et al.*[17] studied the influence of the trialkoxysilane headgroups on reactivity, and product morphology. Their findings indicate a strong dependence of the size of the silyl headgroup on gelation time.

Reaction conditions[5] accompanying the sol–gel process, such as the ratio of water to alkoxysilane,[4,22–24] and the solvent used,[22,23,25,26] have been shown to determine the rates of hydrolysis and condensation,[27] and subsequently dictate the morphology of the solids formed.[4] The water/silane ratio in solution has a significant influence on gelation times,[4,22] and is proportional to the rate of hydrolysis.[28,29] As a result, water content determines the kinetics of polycondensation,[24] and the solids formed differ in their microstructure[28] and pore size distribution.[4,30]

In spite of the many studies of alkoxysilanes used in sol–gel processes, the processes of polycondensation, clusterization, and cluster growth are not well understood at the molecular level. Reactive molecular dynamics simulations can be used to study the influence of sol–gel process variables with atomistic resolution. This will provide insight to the mechanisms of polycondensation, and aid in the engineering of gels with tailored properties.

Department of Chemical Engineering & Materials Science, University of California, Davis 95616, CA, USA. E-mail: rfaller@ucdavis.edu, jddeetz@ucdavis.edu

† Electronic supplementary information (ESI) available: Additional figures relating to all systems simulated in this study. See DOI: 10.1039/c5sm00964b

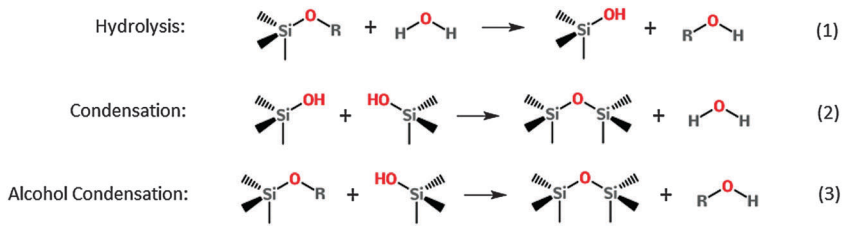

Scheme 1 Reaction equations for hydrolysis, condensation, and alcohol condensation of alkoxysilanes.

To date reactive molecular dynamics studies[14,24,31–34] have modeled the polycondensation of pure hydroxysilanes, or in solutions in pure water. However, in practice precursor solutions contain a mixture of alkoxysilane, solvent[1,15,27] and water. By only considering hydroxysilanes, these studies do not account for modeling the hydrolysis reaction, which under neutral conditions is the rate limiting step[35] in polycondensation. As mentioned above, typical precursor solutions contain mixtures of alkoxysilane, solvent, and water,[5,22] and these compositions have not been considered.

In this study we use a recently parameterized[36] version of a reactive force field, ReaxFF[37,38] to model the early stages of polycondensation in sol–gel systems containing alkoxysilanes, methanol, and water under neutral pH conditions. A baseline system of tetramethoxysilane is modeled and compared to other precursor alkoxysilanes. To determine the impact of silyl headgroups on the morphology of condensed clusters and kinetics of hydrolysis and condensation, we model trimethoxysilane and methyltrimethoxysilane, which have hydrogen and methyl headgroups respectively. Fig. 1 shows the chemical structure of the monomers simulated here. The polycondensation of tetraethoxysilane is modeled in order to study the impact of alkoxy ligand size. Several precursor, water, and alcohol concentrations are modeled to elucidate the impact of precursor solution composition on polycondensation. The structural evolution of siloxane clusters is studied in order to draw correlations between monomer structure and solution composition with the resulting morphology of the products. To our knowledge, this is the first reactive molecular dynamics study of alkoxysilane polycondensation.

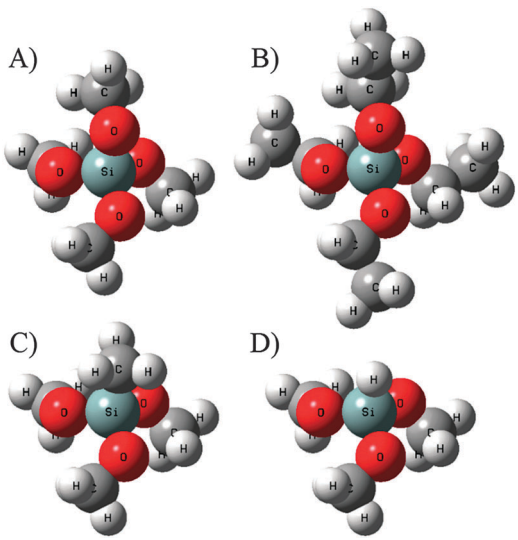

Fig. 1 Chemical structure of the alkoxysilanes studied in this paper: (A) tetramethoxysilane (TetraMS), (B) tetraethoxysilane (TetraES), (C) methyltrimethoxysilane (MethylTriMS), and (D) trimethoxysilane (TriMS).

II. Methods

IIa. Simulation procedure

All simulations were performed using the LAMMPS[39,40] molecular dynamics package in the *NVT* ensemble. The velocity-Verlet integration scheme was used with a timestep of 0.5 fs. Temperature was maintained at 2000 K using the Nosé–Hoover thermostat[41,42] with a time damping constant of 50 fs. The temperatures used in this study are elevated to accelerate hydrolysis and condensation reactions so that they occur on the ns timescale. The use of elevated temperatures is common to reactive molecular dynamics studies[14,24,31,33,34] of the formation of siloxanes due to the high activation energies[43] of hydrolysis and condensation.

To model chemical reactions, a reactive force field, ReaxFF,[37,38] was used. We use our recently parameterized version[36] of ReaxFF for alkoxysilanes. For computational efficiency, we have increased the timestep to 0.5 fs by changing the masses of the hydrogen atoms to 3 amu. It was found that the reaction kinetics are not affected by this change.

The initial positions of the molecules in the simulation box are determined by Packmol,[44] which randomly places them in a simulation box avoiding unphysical overlap. Simulation boxes have volumes ranging from 59.9 nm^3 to 140.9 nm^3 (Table 1). The size of each simulation box is calculated from a weighted average of each molecules pure liquid density under ambient conditions.

Each system was simulated for 5 ns. We constrain all bonds which do not participate in hydrolysis or condensation as it has been shown[45] using reactive force fields that PDMS can decompose and form methane and hydrogen gas. These reactions are not the object of our study. Therefore, all silicon–hydrogen, silicon–carbon, carbon–carbon, oxygen–carbon bonds and carbon–hydrogen bonds are restrained to 1.48, 1.96, 1.54, 1.43, and 1.10 Å respectively using a harmonic bond potential with a coefficient of 50.0 kcal $(mol\ Å^2)^{-1}$.

IIb. Measurement of concentrations, reaction events, and siloxane structure

To monitor the concentrations of chemicals and detect chemical reactions, the bond order[46] between all pairs of atoms

Table 1 Precursor solution compositions

Precursor	Composition precursor : methanol : water	System size (nm^3)
Tetramethoxysilane (TetraMS)	1 : 4 : 4, 1 : 8 : 4, 1 : 12 : 4, 1 : 4 : 8, 1 : 4 : 12, 1 : 8 : 8, 1 : 12 : 12	63.2–140.9
Trimethoxysilane (TriMS)	1 : 4 : 4	59.9
Methyltrimethoxysilane (MethylTriMS)	1 : 4 : 4	62.4
Tetraethoxysilane (TetraES)	1 : 4 : 4	75.7

was analyzed according to the methodology detailed below. In ReaxFF the bond order is defined as:

$$BO_{ij} = \exp\left[-\alpha_\sigma\left(\frac{r_{ij}}{r_\sigma}\right)^{\beta_\sigma}\right] + \exp\left[-\alpha_\pi\left(\frac{r_{ij}}{r_\pi}\right)^{\beta_\pi}\right] + \exp\left[-\alpha_{\pi\pi}\left(\frac{r_{ij}}{r_{\pi\pi}}\right)^{\beta_{\pi\pi}}\right] \quad (1)$$

The total bond order BO_{ij} is a sum of exponentials representing the σ-, π-, and ππ-bonds. The parameters α, β, and r, are used to compute the order of each of these bonds. Each of the exponentials in eqn (1) scales from zero to unity, depending on the interatomic distance, r, between atoms i and j.

In order measure the concentration of chemical groups in the simulation, and detect reactions, the oxygen atoms are tracked and assigned a state depending on the two atoms they share the highest bond order with. By inspecting the reactions detailed in Scheme 1, each of the reactant and product molecules are differentiated by the two elements each oxygen atom is bonded with. For instance, the alkoxysilane state is detected if an oxygen atom is bonded to a silicon and a carbon atom. The number of alkoxysilane (Si–O–C), alcohol (C–O–H), silanol (Si–O–H), and siloxane (Si–O–Si) chemical groups are determined by the two bonds to the oxygen atom which have the highest bond order and the elements of the corresponding atoms.

After the chemical species belonging to each oxygen atom in the system have been determined for each timestep, reactions events are detected by instances in which oxygens change species. For instance, when an oxygen atom switches from water (H–O–H) to silanol (Si–O–H) a hydrolysis reaction has taken place. When silanol (Si–O–H) switches to siloxane (Si–O–Si), a condensation reaction has taken place. In order to avoid a flip-flopping transition state artificially increasing reaction rates, a reaction event is only counted if the atoms bonding to the oxygen in the new state are not the same as it was bonded to in the previous configuration.

The morphology of condensed clusters is determined by the silicon atoms belonging to condensed siloxane bridges. Through a list of siloxane bridges, the average number of bridges per silicon atom and cluster sizes are determined at each step. Additionally, Perlmol[47] is used to implement a siloxane ring-finding algorithm[48,49] which assembles the SSSR (smallest set of smallest rings) at each timestep.

III. Results and discussion

The polycondensation of a baseline system consisting of 100 tetramethoxysilane (TetraMS), 400 methanol, and 400 water molecules is discussed in Section IIIa. Each of the other systems in Table 1 is a mixture of alkoxysilane, methanol, and water. In Section IIIb, the baseline system is compared to solutions containing identical molar ratios of water and methanol, but with different monomers: trimethoxysilane (TriMS), methyltrimethoxysilane (MethylTriMS), and tetraethoxysilane (TetraES). In Section IIIc, several solutions containing different solution compositions of TetraMS, methanol, and water are compared.

IIIa. Modeling polycondensation in methanolic tetramethoxysilane precursor solution

In this section we discuss the polycondensation of a tetramethoxysilane (TetraMS) baseline system. The initial concentrations of TetraMS, methanol, and water in this solution are 2.62, 10.5, and 10.5 M respectively. Fig. 2 shows the concentrations of chemical species as a function of time normalized by the initial concentration of alkoxysilane groups (Si–O–C). Over 5 ns of simulation time, the precursor concentration decreases by over sixty percent, while the number of siloxane bridges increases. This indicates the alkoxysilanes are condensing to siloxane bridges. The concentration of all components in Fig. 2 is consistent with the stoichiometry in Scheme 1. The concentration of methanol increases proportionally with the depletion of precursor, accompanied by a slight consumption of water. Fig. 2 does not show an appreciable growth in the concentration of silanol (Si–O–H). It has been shown that at neutral pH hydrolysis (Reaction (1) in Scheme 1) is the rate limiting step to polycondensation.[13,35] Thus, silanol species do not have a significant presence at this pH.

Multiple replicas of the baseline system were simulated by differently randomizing the initial positions of the molecules.

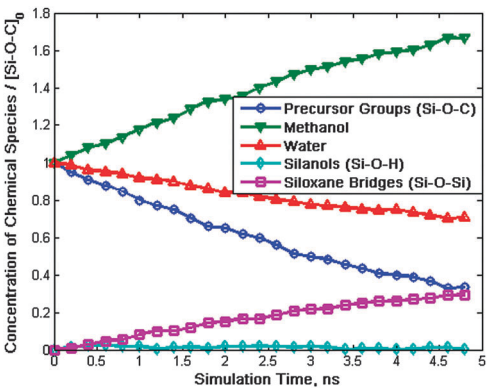

Fig. 2 Concentration of chemical groups in system normalized by the initial number of alkoxysilane groups. The initial system composition is a 1 : 4 : 4 molar ratio of TetraMS, methanol, and water.

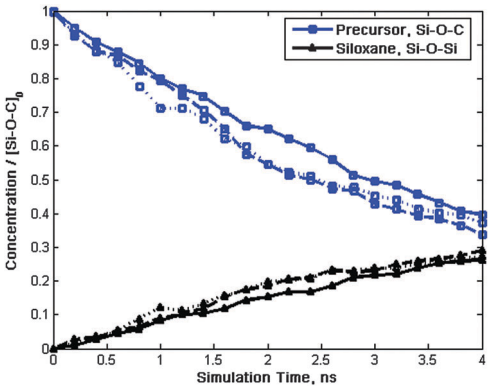

Fig. 3 Concentration of precursor and siloxane chemical groups in system normalized by the initial number of alkoxysilane groups. Multiple simulation runs, each with randomized initial positions and coordinates, are shown as the solid, dashed, and dotted lines.

The concentration profiles of alkoxysilane (Si–O–C) and siloxane (Si–O–Si) groups for the three replications of the baseline system are shown in Fig. 3. The profiles do not show much difference and follow the same trends as Fig. 2. Variations in the concentrations of various reactants and products are expected of a small system due to the random nature of molecular collisions and nucleation of siloxane clusters.

The distribution of Si atoms with different numbers of siloxane bridges is shown in Fig. 4. Fully condensed silicon atoms from TetraMS have four bridges. As monomers condense and form siloxane bridges, the percentage of uncondensed silicon atoms decreases. Silicons with one siloxane bridge dominate from around 0.5 ns to 2.5 ns, making up around 25 percent of all silicon atoms. Silicons with two bridges become the most common species around 3.5 ns. At this time, three-bridged and four-bridged silicons are also present, and ninety percent have at least one bridge. After 5 ns, seventy percent of silicon atoms have two or three siloxane bridges. Fig. 4 demonstrates the progressive evolution of more highly bridged species. Single bridged species form quickly. Three and four bridged silicon species are formed more slowly. This is most likely due to the slower diffusion of

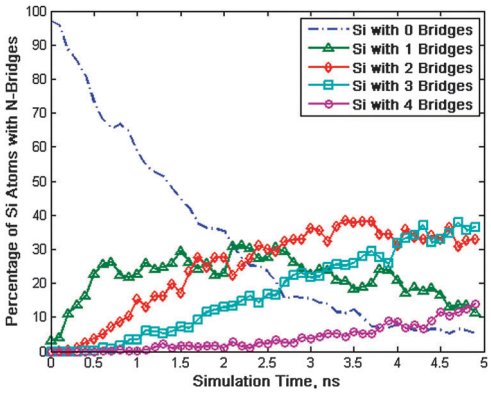

Fig. 4 Distribution of silicon atoms with different numbers of condensed siloxane Si–O–Si bridges. The initial system composition is a 1 : 4 : 4 molar ratio of TetraMS, methanol, and water.

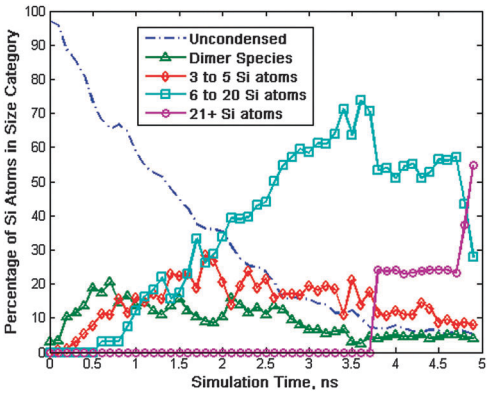

Fig. 5 Siloxane cluster size distribution for system with initial composition of a 1 : 4 : 4 molar ratio of TetraMS, methanol, and water.

clustered species, reduced quantities of precursor monomer, and reduced steric accessibility of reacting groups. The general characteristics of Fig. 4 (*i.e.* the progressive evolution of higher-bridged silicon atoms with increasingly longer timescales of condensation to form these species) are observed in simulation[14,24,32,50,51] and NMR[10,16] studies.

The siloxane cluster size distribution is illustrated in Fig. 5. At around 0.5 ns mostly dimers are formed, with a small number of clusters containing three to five silicon atoms. As further condensation takes place and more siloxane bridges are formed, progressively larger clusters are generated. Around 3.5 ns into the simulation, clusters containing between six and twenty silicon atoms are the most frequent, accounting for around seventy percent of silicons. At 4.8 ns the percentage of silicon atoms in this size category sharply drops, leading to the formation of clusters with more than twenty silicon atoms. The sharp drops in the percentage of clusters between six and twenty silicon atoms shown in Fig. 5 can be associated with cluster–cluster aggregation. The timescales of cluster formation are slower than those for hydroxysilane clusterization[14] due to the added hydrolysis step, which limits siloxane nucleation. For condensation to occur, hydrolysis must first form silanol.

Fig. 6 shows the evolution of the largest siloxane cluster size for the three replications shown in Fig. 3. With increasing simulation time, the size of the largest siloxane cluster grows. At early reaction times siloxane dimers are formed which can subsequently grow with the addition of monomers. Monomer addition is the dominant growth mechanism in the beginning stages of polycondensation. With longer timescales, cluster–cluster aggregation events are observed. Sudden large increases in the maximum cluster size in the simulation box indicate the fusion of clusters. One interesting aspect of Fig. 6 is that it portrays the stochastic nature of cluster–cluster aggregation. With neutral pH, the hydrolysis reaction is the rate-limiting step to polycondensation. Thus, silanol species will have low concentration, and there will be subsequently fewer monomers able to nucleate to form siloxane clusters. The development of siloxane clusters depends on these random events, which partially explains the differences observed between the replications in Fig. 6. The time between random collisions of clusters influences

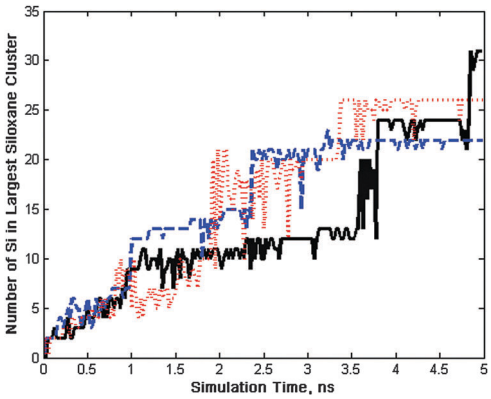

Fig. 6 Maximum siloxane cluster size for system initially containing a 1 : 4 : 4 molar ratio of TetraMS, methanol, and water. Multiple simulation runs, each with randomized initial positions and coordinates, are shown as the solid, dashed, and dotted lines. Cluster growth and cluster–cluster aggregation is observed.

the timescales of cluster–cluster aggregation events. As our simulations only have a few such large clusters, aggregation is significantly influenced by random collisions.

Although there are differences between the maximum cluster sizes, the systems depict similar behavior in which cluster growth is dominated by monomer addition at small time scales, and cluster aggregation at later times.

Fig. 7 shows the percentages of silicon atoms in siloxane rings, as well as condensed silicon atoms that do not participate in rings. At 0.5 ns, condensed species are formed, but very few rings are present. At this time, mainly dimers and linear clusters are formed. Around 2.5 ns, nearly half of the silicon atoms in the system are condensed, but do not belong to any siloxane ring, while a third of silicon atoms have already condensed to rings. By 5 ns eighty percent of the silicon atoms belong to siloxane rings and the average cluster size is greater than ten, and most silicon atoms have at least two siloxane bridges. The fluctuations in the percentages of condensed non-ring silicon correspond to the ring closure and cleavage reactions. Siloxane rings formed from condensation of hydroxysilanes have been predicted by Monte Carlo[50,51] and molecular dynamics[14,24,32] simulations to

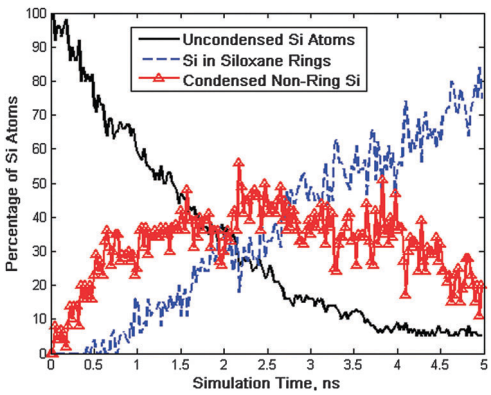

Fig. 7 Percentage of silicon atoms which are uncondensed, condensed in siloxane rings, or condensed but not in rings in a system with an initial composition of a 1 : 4 : 4 molar ratio of TetraMS, methanol, and water.

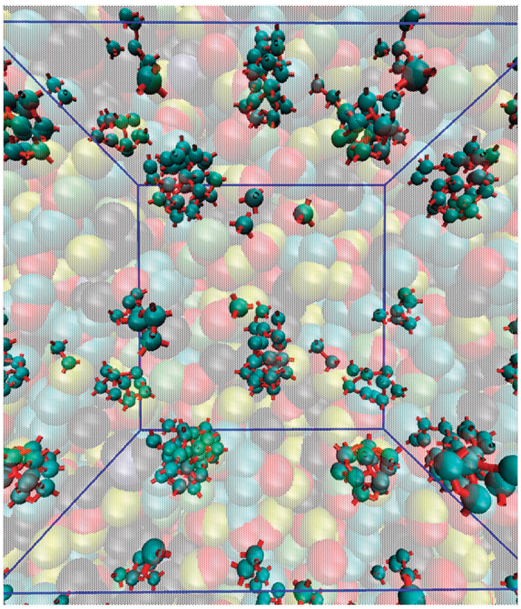

Fig. 8 Simulation snapshot of silicon (spheres) and oxygen atoms (sticks) after 5 ns from a system with initial composition of 100 TetraMS, 400 water, and 400 methanol molecules. The solvent and other atoms are represented by the faint background.

have four to five silicon atoms. In this work, after 5 ns, the average number of silicon atoms in each siloxane ring is predicted to be about 4.2. Rings containing four silicon atoms are the most frequent, representing a third of all siloxane rings.

A snapshot of the simulation after 5 ns is depicted in Fig. 8. The representation consists of spheres, showing the positions of silicon atoms, and sticks, showing the positions of silicon–oxygen bonds. The majority of silicon atoms have polymerized into small clusters. This representation consists only of the condensed siloxane skeleton. This molecular graphic was constructed using VMD 1.9.2.[52]

These simulations have only taken place during the early stages of polycondensation, in which alkoxysilanes form small siloxane clusters. In experiments, siloxane clusters grow in a sol to reach sizes varying from 1–100 nm[53] in diameter depending on the reaction conditions. The internal structure of the sol particles, whether they are loosely networked or densely rigid, will be influenced by the process of polycondensation. For neutral pH, the hydrolysis is rate limiting, which inhibits particle ripening in the siloxanes. On the timescales of cluster growth, this allows for the siloxane particles to form dense internal structures prior to gelation. Although these simulations run only for five nanoseconds, it is anticipated that the effects observed on polycondensation will influence sol formation, gelation, and hence the final morphology of the silicate matrix developed.

IIIb. Effects of alkoxysilane chemical structure: silyl headgroups and alkoxy ligands

Polycondensation is compared between four different alkoxysilane monomers: tetramethoxysilane (TetraMS), trimethoxysilane (TriMS),

Table 2 Summary of polycondensation characteristics for different precursor monomers

		After 5 ns of simulation time				
Precursor identity	$k_{hydrolysis}$, L (mol ns)$^{-1}$	Percent (Si–O–C) remaining	Percent of Si atoms condensed	Number of Si–O–Si per Si atom	Number of Si atoms per ring	Percent of Si atoms in rings
TetraMS	0.0191	31.8	95	2.41 ± 1.07	4.60 ± 1.64	76
TriMS	0.0267	14.7	87	2.05 ± 1.09	3.77 ± 1.57	62
MethylTriMS	0.0149	38.0	88	1.74 ± 0.96	3.92 ± 0.76	35
TetraES	0.0127	51.0	80	1.66 ± 1.04	4.10 ± 1.51	50

methyltrimethoxysilane (MethylTriMS), and tetraethoxysilane (TetraES) at equivalent water and methanol dilutions as shown in Table 1. A summary of the characteristics of polycondensation for each monomer is contained in Table 2. A reaction rate coefficient for hydrolysis was derived from the initial disappearance rate of alkoxysilane groups (Si–O–C), according to eqn (2):

$$k_{\text{hydrolysis}} = \frac{\mathrm{d}[\text{SiOC}]}{\mathrm{d}t}(0) \Big/ \left([\text{SiOC}]_0[\text{H}_2\text{O}]_0\right) \qquad (2)$$

This formulation assumes the rates of the alcohol condensation and the reverse reactions are negligible at low reaction time. These are valid assumptions due to the low concentration of silanol at the beginning stages. Temporal characteristics of polycondensation, such as the percent alkoxysilane remaining are presented in Table 2 after five nanoseconds.

Fig. 9 shows the concentration of alkoxysilane for each system. The initial rate coefficient for hydrolysis in Table 2 indicates that the depletion of alkoxide groups occurs most quickly for TriMS. Compared to the molecular structure of TetraMS, the TriMS monomer has a hydride group attached to the silicon atom in the place where TetraMS has a methoxy group. This small hydrogen group offers little shielding to the central silicon atom from nucleophilic attacks by an approaching water. Conversely, the bulky methyl and ethoxy groups attached to MethylTriMS and TetraES slow the reaction of the alkoxy groups by blocking water. The depletion of alkoxysilane groups is slightly slower for MethylTriMS than for TetraMS, which is explained by the bulky methylsilane close to the central silicon atom. The hydrolysis of the ethoxysilane (TetraES) groups occurs more slowly than for methoxysilane (TetraMS), likely due to the steric bulk of the former.

The hydrolysis rate coefficient is correlated with the percentage of unreacted alkoxysilane chemical groups after five nanoseconds of simulation time. More than eighty-five percent of the TriMS molecules have reacted by this time. TetraES is the slowest to react, with only around fifty percent of its alkoxy groups reacted after 5 ns. In spite of the alkoxy groups of TriMS hydrolyzing more quickly than TetraMS, a smaller percentage of silicon atoms of the TriMS monomers have condensed after 5 ns, which implies these monomers are hydrolyzed, but have not condensed yet.

The average number of siloxane (Si–O–Si) bridges per silicon atom is shown in Table 2. As shown in Fig. 4, the average number of bridges per silicon atom increases with simulation time. After 5 ns, the system containing TetraMS has the greatest number of siloxane bridges per silicon atom. Due to the presence of silyl headgroups of TriMS and MethylTriMS, there are fewer potential bridging sites. Thus, trialkoxides are expected to form solids with fewer siloxane bridges. MethylTriMS does not react as quickly as TriMS. The silicon atoms of the TriMS system are more highly bridged with siloxane after 5 ns. The distribution of siloxane bridges of TriMS is shown in Fig. 10. Compared with the evolution of bridges for TetraMS shown in Fig. 4, the formation of silicon atoms with two and three bridges occurs slightly faster for TriMS. Additionally, saturation of silicon with siloxanes (three bridges for TriMS, four for TetraMS), occurs much more quickly for TriMS.

Fig. 11 shows the percentage of silicon atoms in rings as well as the percentage of condensed silicon. A similar percentage of

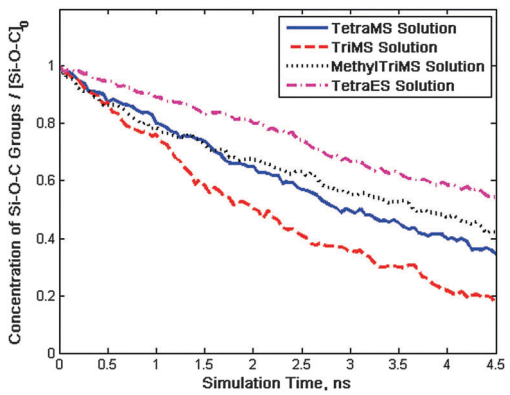

Fig. 9 Concentration of alkoxysilane groups (Si–O–C) in different systems (TetraMS, TriMS, MethylTriMS, TetraES) normalized by the initial number of alkoxysilane groups.

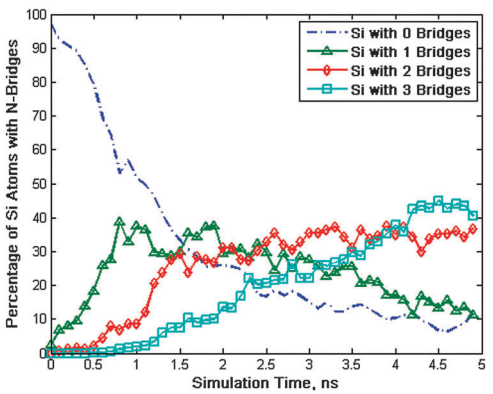

Fig. 10 Distribution of silicon atoms of trimethoxysilane with different numbers of condensed siloxane Si–O–Si bridges. The initial system composition is a 1 : 4 : 4 molar ratio of TriMS, methanol, and water.

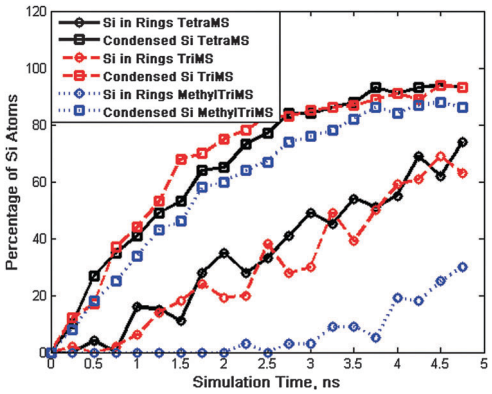

Fig. 11 Percent of silicon atoms condensed compared with the percent in siloxane rings.

silicon atoms for TriMS and TetraMS exist in condensed siloxane rings. For the MethylTriMS a lower percentage of silicon atoms exists in siloxane rings, which indicates that MethylTriMS may have a preference for more branched structures, as opposed to TriMS and TetraMS. This is due to the steric bulk of the methyl headgroup, which interferes with the formation of siloxane bridges and rings. Ring formation also occurs more slowly for TetraES than it does for TetraMS, which is ascribed to the slower hydrolysis rate of the alkoxy groups. Interestingly, all of the precursor molecules form siloxane rings of different sizes, as indicated by Table 2. In comparison to other precursor monomers, the siloxane ring size of MethylTriMS follows a more narrow distribution. This might be due to the size of the methyl headgroup.

In comparison to TetraMS, the polycondensation of TriMS occurs more aggressively, owing to the small size of the hydrogen headgroup as seen in increased rates of hydrolysis and condensation. Loy *et al.*[17] indicates longer gelation times for solutions containing TetraMS and TetraES when compared with TriMS and triethoxysilane.

Ethoxysilane groups are depleted markedly slower than methoxysilanes. These differences can be attributed to the limited accessibility of the central silicon atom of TetraES due to the larger ligand size. The development of siloxane bridges for TetraES is much slower compared to TetraMS, but it is not clear if this difference manifests due to steric hindrance of the ethoxy groups, or by reduced diffusion owing to the larger size of the monomer. It has been indicated in literature that the kinetics of polycondensation of TetraES is slower[11,17] than that of TetraMS. Loy *et al.*[17] found longer gelation times for ethoxysilanes under neutral and acidic conditions when compared to methoxysilanes.

The timescale of these simulations is only for the early stages of polycondensation, but it is expected that the characteristics of the siloxane clusters formed will influence the structure of sol particles developed prior to gelation. Hence, the physical properties of the gel produced from the sol–gel process will be determined by the nature of polycondensation. Due to the lower number of bridging sites on methyltrimethoxysilane and trimethoxysilane, it is expected that they will form clusters which are loosely bound with siloxane bridges that lower elastic moduli than solids developed from tetra-alkoxysilanes. Due to the interference of the methyl headgroup with the formation of siloxane bridges and rings, methyltrimethoxysilane is expected to have a longer gelation time and to produce siloxanes with a greater uniformity in siloxane rings (as demonstrated in Table 2), such as silsesquioxanes.[16]

The rate of polycondensation of tetraethoxysilane is slower than tetramethoxysilane. The bulky ethoxy group sterically hinders hydrolysis by blocking access to the central silicon atom. By slowing hydrolysis, there are fewer nucleation events in solution. This results in the formation of larger sol particles as these nuclei consume all of the monomers in the solution. After gelation solids with larger pore diameters will be formed.

IIIc. Effects of alkoxysilane, water, and alcohol composition in solution

Different solution compositions of tetramethoxysilane (TetraMS), methanol, and water were simulated. As discussed in IIIa, a 1 : 4 : 4 molar ratio of TetraMS : methanol : water was used as a baseline system for comparison to other solution compositions. In order to determine the effect of changing the water composition in solution, the initial molar ratio of TetraMS : methanol : water is varied from 1 : 4 : 4 to 1 : 4 : 8 and 1 : 4 : 12. The effects of methanol content on polycondensation is determined by comparing the 1 : 4 : 4 ratio system with 1 : 8 : 4 and 1 : 12 : 4 systems. Lastly, the impact of alkoxysilane concentration is probed by modeling three systems with different levels of tetramethoxysilane dilution: the 1 : 4 : 4, 1 : 8 : 8, and 1 : 12 : 12 systems.

Table 3 summarizes the characteristics of polycondensation for each of these compositions. Quantities which depend on reaction time in Table 3 are presented as their value after five nanoseconds of simulation time. The reaction rate coefficients calculated using eqn (2) are nearly equivalent for all compositions. This means that the concentrations of alcohol, water, and silane at our compositions do not have as pronounced of an effect of the reaction rate coefficient as the chemical structure of the precursor molecule does (Table 2).

The concentration of water has a pronounced effect on the kinetics of polycondensation. By increasing the ratio of H_2O : TetraMS from 4 : 1 to 8 : 1 to 12 : 1, there are clear differences in the rates of hydrolysis and condensation. As water concentration increases, the percent of alkoxysilane (Si–O–C) remaining in the simulation box decreases at a much faster rate. The average number of siloxane bridges per silicon atom and the percent of silicon atoms in siloxane rings both increase. It has been shown previously[28] that increasing the ratio of water to precursor monomer promotes hydrolysis and condensation. Fig. 12 shows the concentration of precursor chemical groups as a function of simulation time. Clearly, the depletion of alkoxysilane in the 1 : 8 : 4 composition is much faster than the 1 : 4 : 4 system. The difference between the 1 : 12 : 4 and 1 : 8 : 4 systems is not as pronounced. This agrees with classical kinetics. At large concentrations of a reactant in a bimolecular second order reaction, the reaction transitions to pseudo first order.

Increasing the H_2O : TetraMS ratio accelerates polycondensation. As hydrolysis is a prerequisite to condensation (Scheme 1),

Table 3 Summary of polycondensation characteristics for different solution compositions

		After 5 ns of simulation time				
TetraMS : methanol : water	$k_{hydrolysis}$, L (mol ns)$^{-1}$	Percent (Si–O–C) remaining	Percent of Si atoms condensed	Number of Si–O–Si per Si atom	Number of Si atoms per ring	Percent of Si atoms in rings
1 : 4 : 4	0.019	31.8	95	2.41 ± 1.07	4.60 ± 1.64	76
1 : 4 : 8	0.022	16.8	100	2.89 ± 0.96	4.15 ± 1.38	92
1 : 4 : 12	0.019	10.2	100	3.08 ± 0.94	4.39 ± 1.43	88
1 : 8 : 4	0.020	40.5	86	1.98 ± 1.15	3.80 ± 1.50	63
1 : 12 : 4	0.022	50.8	83	1.63 ± 1.12	3.93 ± 1.39	33
1 : 8 : 8	0.020	28.3	95	2.48 ± 0.99	4.08 ± 1.64	73
1 : 12 : 12	0.018	28.3	94	2.46 ± 1.02	4.10 ± 1.66	79

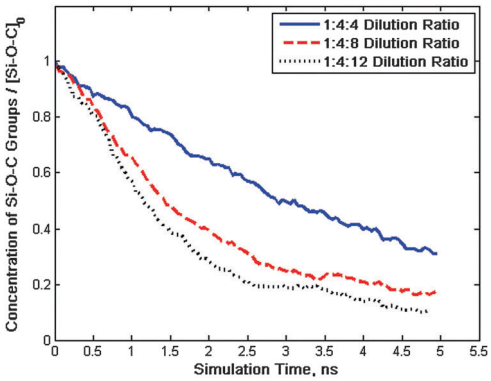

Fig. 12 Normalized concentration of alkoxysilane groups (Si–O–C) in different systems (1 : 4 : 4, 1 : 4 : 8, and 1 : 4 : 12 tetramethoxysilane : methanol : water). Concentration is normalized by the initial number of alkoxysilane groups.

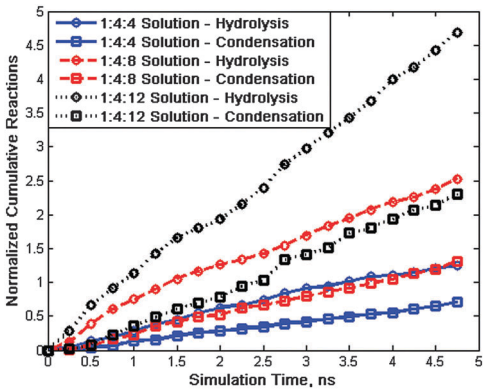

Fig. 13 Cumulative hydrolysis and condensation reactions normalized by initial number of alkoxysilane groups.

accelerating hydrolysis will accelerate condensation. Fig. 13 shows the cumulative number of hydrolysis and condensation reactions during the simulation. Increasing water concentration proportionally increases the rates of hydrolysis and condensation at higher concentrations. Although the time derivative of the concentration profiles shown in Fig. 12 begin to decrease, indicating an approach to equilibrium, the frequency of hydrolysis and condensation reactions do not slow down according to Fig. 13. This indicates that at equilibrium there is competition among forward and reverse reactions which allows further hydrolysis and condensation to take place.

Rao and Gelb[24] have shown that increasing the water to silicon ratio resulted in accelerating the rate at which the silicon atoms are saturated with siloxane bridges. After 5 ns, the 1 : 4 : 4, 1 : 4 : 8 and 1 : 4 : 12 compositions have 2.4, 2.9, and 3.1 siloxane bridges per silicon atom respectively. As the maximum number of available bridging sites available to TetraMS is four, this implies a high degree of condensation for all solutions.

Ring formation is facilitated at high water concentrations. The average size of siloxane ring as a function of simulation time is shown in Fig. 14. The average ring size in the 1 : 4 : 4, 1 : 4 : 8, and 1 : 4 : 12 compositions is qualitatively similar. Initially small two membered rings are formed, but are soon replaced by larger rings. Over the course of the simulation, the average size of siloxane rings increases. Two-membered rings have excess strain[54] from the O–Si–O and Si–O–Si angles. The average size of siloxane rings increases over time as additional monomers are available to form rings. Five-membered rings have been reported as the most frequent from hydroxysilanes simulations.[14,24,32] It has also been shown that the average number of silicon atoms per siloxane ring increases[32] over the course of polycondensation. Although the simulations are not equilibrated after 5 ns, it is clear the average ring size at all H_2O : TetraMS ratios have more than four silicons.

Changing the molar ratio of the alkoxysilane:methanol in our simulations from 1 : 4 to 1 : 12 slows the depletion of methoxysilane groups. Siloxane bridges are formed more quickly in the 1 : 4 : 4 mixture than for the 1 : 8 : 4 and 1 : 12 : 4 systems. High methanol : TetraMS ratios have been reported elsewhere to increase gelation times[22] and promote esterification of alcohol with silanol.[5,29] There is a dilution effect in which methanol reduces the concentration of reactant methoxysilane and water. Low molar ratios of alcohol to precursor monomer have been shown[28] to promote hydrolysis during the early stages of polycondensation. Alcohol solvents have been shown[29,55] to engage in re-esterification reactions in which alcohol can react with silanol to form alkoxysilane. The number of siloxane bridges per silicon increases most slowly in Table 3 for the 1 : 12 : 4 system. Ring formation occurs more slowly for solutions with high methanol : TetraMS ratios.

We have already shown that increasing water concentration accelerates hydrolysis and condensation, whereas increasing methanol slightly inhibits reactions. By changing the TetraMS : methanol : water solution composition from 1 : 4 : 4 to 1 : 8 : 8 and 1 : 12 : 12, the concentration of TetraMS is reduced. In spite

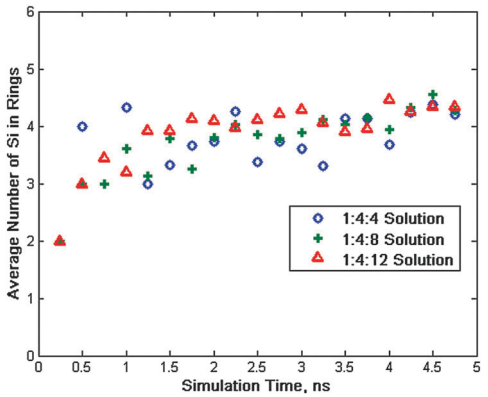

Fig. 14 Average number of silicon atoms in each siloxane ring for the 1 : 4 : 4, 1 : 4 : 8, and 1 : 4 : 12 systems.

of the increase in methanol concentration, methoxysilanes are hydrolyzed more quickly at 1 : 8 : 8, and siloxane bridges form faster. The reaction rates are slightly faster for 1 : 8 : 8 than for 1 : 8 : 4, but much slower than 1 : 4 : 8. It is possible that alcohol hydrogen bonds with the excess water preventing its reaction with alkoxysilane.

Hydrolysis and condensation are greatly accelerated for 1 : 4 : 8 compared to 1 : 4 : 4. Adding methanol to the 1 : 4 : 8 system to form the 1 : 8 : 8 slows polycondensation, either by diluting the precursor monomers, or by esterification of the silanols generated from hydrolysis. A reverse esterification reaction has been shown[29] to inhibit condensation in this manner.

Although these simulations only last five nanoseconds and have clearly not equilibrated, some of the characteristics of polycondensation are expected to influence the structure of the siloxane gel. High H_2O : Si ratios accelerate the rate of the hydrolysis reaction, which leads to a higher concentration of silanol, and the formation of a greater number siloxane nuclei than at low water concentrations. The ratios between the maximum and average siloxane cluster sizes after 5 ns for the 1 : 4 : 4 and 1 : 4 : 8 dilutions are 2.7 and 1.5 respectively. If this trend is continued consuming all remaining monomer, the 1 : 4 : 8 dilution will form smaller clusters, compared to the 1 : 4 : 4 solution, leading to the formation of a gel with high surface area.

IV. Conclusions

Reactive molecular dynamics has been used to study the polycondensation of alkoxysilane systems. We have used ReaxFF to investigate the hydrolysis and condensation reactions of systems containing alkoxysilane, alcohol, and water. In principle, this force field is not limited to the specific molecules we have modeled and could be extended to simulating the polycondensation of other monomer alkoxysilanes, and solutions containing other solvents.

Both hydrolysis and condensation reactions were observed in all solutions. The rates of reaction of trialkoxysilanes correlates directly with the size of their silyl headgroups. The small size of the hydrogen headgroup of trimethoxysilane offers little resistance to hydrolysis by water molecules. In contrast, the bulky nature of the methyl headgroup of methyltrimethoxysilane impedes it. The condensation reaction appears to be more significantly affected by steric hindrance than hydrolysis. The steric bulk of the methyl headgroup inhibits the formation of completely condensed silicon atoms, as the monomers of methyltrimethoxysilane are slower to form siloxane bridges and rings.

The effects of alkoxy ligand size were studied by modeling systems of tetramethoxysilane tetraethoxysilane with equivalent amounts of alcohol and water. Polycondensation was slower for the ethoxy solution, although it isn't clear whether this is due to slower diffusion of the alkoxysilane monomer, or steric hindrance of the ethoxy ligands.

The 1 : 4 : 4 molar composition of precursor : methanol : water was diluted with water and methanol to form the 1 : 4 : 8, 1 : 4 : 12, 1 : 8 : 4, 1 : 12 : 4, 1 : 8 : 8, and 1 : 12 : 12 solutions. Increasing the water : silane ratio increases the rates of hydrolysis and condensation. Saturation of silicon atoms with siloxane bridges and ring closure are also accelerated at high water concentrations. Increasing water content in the precursor solution accelerates cluster growth. Systems containing different concentrations of tetramethoxysilane were modeled with the 1 : 4 : 4 and 1 : 8 : 8 systems. The higher water concentration of the 1 : 8 : 8 and 1 : 12 : 12 systems accelerates the kinetics of hydrolysis and condensation.

In all systems, it is seen that although the concentration profiles of precursor (Si–O–C) chemical groups and siloxane (Si–O–Si) bridges begin to approach equilibrium, the rates of hydrolysis and condensation do not decrease. This implies that, at equilibrium, forward and reverse reactions will be competing such there are no significant changes to the concentrations of chemical components of the system.

Polycondensation has been explored under neutral conditions in this study, but often basic or acidic pH are used to catalyze reactions. Our results are limited to the initial stages of the sol–gel process. Morphological effects resulting from varying rates of diffusion, hydrolysis, and condensation could be seen more clearly over longer timescales and lengthscales.

Acknowledgements

This paper has benefited from fruitful discussions with Dr Nerissa Draeger, Dr Peter Woytowitz, and Dr Ronald Pearlstein. The authors are grateful for funding provided by Lam Research Corporation.

References

1 C. J. Brinker and G. W. Scherer, *Sol–gel science: the physics and chemistry of sol–gel processing*, Gulf Professional Publishing, 1990.
2 M. Schmidt and F. Schwertfeger, *J. Non-Cryst. Solids*, 1998, **225**, 364–368.
3 M. T. Anderson, P. S. Sawyer and T. Rieker, *Microporous Mesoporous Mater.*, 1998, **20**, 53–65.

4 M. Stolarski, J. Walendziewski, M. Steininger and B. Pniak, *Appl. Catal., A*, 1999, **177**, 139–148.
5 K. Sinkó, *Materials*, 2010, **3**, 704–740.
6 W. F. Zeno, S. Hilt, K. K. Aravagiri, S. H. Risbud, J. C. Voss, A. N. Parikh and M. L. Longo, *Langmuir*, 2014, **30**, 9780–9788.
7 S. Seraji, Y. Wu, M. Forbess, S. J. Limmer, T. Chou and G. Cao, *Adv. Mater.*, 2000, **12**, 1695–1698.
8 E. P. Plueddemann, *Silane coupling agents*, Springer, 1982.
9 H. Schmidt, H. Scholze and A. Kaiser, *J. Non-Cryst. Solids*, 1984, **63**, 1–11.
10 A. Vainrub, F. Devreux, J. Boilot, F. Chaput and M. Sarkar, *J. Mater. Sci. Eng. B*, 1996, **37**, 197–200.
11 B. Tan and S. E. Rankin, *J. Phys. Chem. B*, 2006, **110**, 22353–22364.
12 T. Bernards, M. Van Bommel and A. Boonstra, *J. Non-Cryst. Solids*, 1991, **134**, 1–13.
13 C. Brinker, *J. Non-Cryst. Solids*, 1988, **100**, 31–50.
14 K. Yamahara and K. Okazaki, *Fluid Phase Equilib.*, 1998, **144**, 449–459.
15 K. Chen, T. Tsuchiya and J. D. Mackenzie, *J. Non-Cryst. Solids*, 1986, **81**, 227–237.
16 L. Matejka, O. Dukh, D. Hlavatá, B. Meissner and J. Brus, *Macromolecules*, 2001, **34**, 6904–6914.
17 D. A. Loy, B. M. Baugher, C. R. Baugher, D. A. Schneider and K. Rahimian, *Chem. Mater.*, 2000, **12**, 3624–3632.
18 R. J. Corriu, D. Leclercq, P. Lefevre, P. Mutin and A. Vioux, *J. Non-Cryst. Solids*, 1992, **146**, 301–303.
19 I. Hasegawa and S. Sakka, *J. Non-Cryst. Solids*, 1988, **100**, 201–205.
20 J. A. Howarter and J. P. Youngblood, *Langmuir*, 2006, **22**, 11142–11147.
21 M. Hu, S. Noda, T. Okubo, Y. Yamaguchi and H. Komiyama, *Appl. Surf. Sci.*, 2001, **181**, 307–316.
22 S. Chang and T. Ring, *J. Non-Cryst. Solids*, 1992, **147**, 56–61.
23 A. V. Rao and N. Parvathy, *J. Mater. Sci.*, 1993, **28**, 3021–3026.
24 N. Z. Rao and L. D. Gelb, *J. Phys. Chem. B*, 2004, **108**, 12418–12428.
25 J. H. Harreld, T. Ebina, N. Tsubo and G. Stucky, *J. Non-Cryst. Solids*, 2002, **298**, 241–251.
26 K. T. Ranjit, I. Martyanov, D. Demydov, S. Uma, S. Rodrigues and K. J. Klabunde, *J. Sol-Gel Sci. Technol.*, 2006, **40**, 335–339.
27 H. Jiang, Z. Zheng and X. Wang, *Vib. Spectrosc.*, 2008, **46**, 1–7.
28 J. Gnado, P. Dhamelincourt, C. Pelegris, M. Traisnel and A. L. M. Mayot, *J. Non-Cryst. Solids*, 1996, **208**, 247–258.
29 J. Pouxviel, J. Boilot, J. Beloeil and J. Lallemand, *J. Non-Cryst. Solids*, 1987, **89**, 345–360.
30 J. C. Ro and J. C. In, *J. Non-Cryst. Solids*, 1991, **130**, 8–17.
31 B. Feuston and S. Garofalini, *J. Phys. Chem.*, 1990, **94**, 5351–5356.
32 S. H. Garofalini and G. Martin, *J. Phys. Chem.*, 1994, **98**, 1311–1316.
33 S. Bhattacharya and J. Kieffer, *J. Chem. Phys.*, 2005, **122**, 094715.
34 S. Bhattacharya and J. Kieffer, *J. Phys. Chem. C*, 2008, **112**, 1764–1771.
35 E. Pope and J. Mackenzie, *J. Non-Cryst. Solids*, 1986, **87**, 185–198.
36 J. D. Deetz and R. Faller, *J. Phys. Chem. B*, 2014, **118**, 10966–10978.
37 A. C. T. van Duin, S. Dasgupta, F. Lorant and W. A. Goddard, *J. Phys. Chem. A*, 2001, **105**, 9396–9409.
38 K. Chenoweth, A. C. T. van Duin and W. A. Goddard, *J. Phys. Chem. A*, 2008, **112**, 1040–1053.
39 S. Plimpton, *J. Comput. Phys.*, 1995, **117**, 1–19.
40 H. M. Aktulga, J. C. Fogarty, S. A. Pandit and A. Y. Grama, *Parallel Comput.*, 2012, **38**, 245–259.
41 S. Nosé, *J. Chem. Phys.*, 1984, **81**, 511–519.
42 W. G. Hoover, *Phys. Rev. A: At., Mol., Opt. Phys.*, 1985, **31**, 1695.
43 S. Okumoto, N. Fujita and S. Yamabe, *J. Phys. Chem. A*, 1998, **102**, 3991–3998.
44 L. Martínez, R. Andrade, E. G. Birgin and J. M. Martínez, *J. Comput. Chem.*, 2009, **30**, 2157–2164.
45 K. Chenoweth, S. Cheung, A. C. T. van Duin, W. A. Goddard and E. M. Kober, *J. Am. Chem. Soc.*, 2005, **127**, 7192–7202.
46 L. Pauling, *The nature of the chemical bond and the structure of molecules and crystals: an introduction to modern structural chemistry*, Cornell University Press, 1960.
47 I. Tubert-Brohman, *PerlMol, version 0.37*, Yale University, 2004.
48 A. R. Leach, D. P. Dolata and K. Prout, *J. Chem. Inf. Comput. Sci.*, 1990, **30**, 316–324.
49 J. Figueras, *J. Chem. Inf. Comput. Sci.*, 1996, **36**, 986–991.
50 A. Malani, S. M. Auerbach and P. A. Monson, *J. Phys. Chem. Lett.*, 2010, **1**, 3219–3224.
51 A. Malani, S. M. Auerbach and P. A. Monson, *J. Phys. Chem. C*, 2011, **115**, 15988–16000.
52 W. Humphrey, A. Dalke and K. Schulten, *J. Mol. Graphics*, 1996, **14**, 33–38.
53 P. Wijnen, T. Beelen, C. Rummens and R. Van Santen, *J. Non-Cryst. Solids*, 1991, **136**, 119–125.
54 R. J. Field and E. W. Olson, *J. Non-Cryst. Solids*, 2001, **285**, 194–201.
55 C. Brinker, K. Keefer, D. Schaefer, R. Assink, B. Kay and C. Ashley, *J. Non-Cryst. Solids*, 1984, **63**, 45–59.